Sciencexpress Reports

Ice Shelf Melting Around Antarctica

E. Rignot,[1,2]* S. Jacobs,[3] J. Mouginot,[1] B. Scheuchl[1]

[1]Department of Earth System Science, University of California, Irvine, CA 92697, USA. [2]Jet Propulsion Laboratory, Pasadena, CA 91109, USA. [3]Lamont-Doherty Earth Observatory, Columbia University, Palisades, NY 10964, USA.

*Corresponding author. E-mail: erignot@uci.edu

We compare the volume flux divergence of Antarctic ice shelves in 2007–2008 with 1979–2010 surface accumulation and 2003–2008 thinning to determine their rates of melting and mass balance. Basal melt of 1325 ± 235 gigatons per year (Gt/year) exceeds a calving flux of 1089 ± 139 Gt/year, making ice shelf melting the largest ablation process in Antarctica. The giant cold-cavity Ross, Filchner, and Ronne ice shelves covering two-thirds of the total ice shelf area account for only 15% of net melting. Half of the meltwater comes from 10 small, warm-cavity southeast Pacific ice shelves occupying 8% of the area. A similar high melt/area ratio is found for six East Antarctic ice shelves, implying undocumented strong ocean thermal forcing on their deep grounding lines.

The Antarctic Ice Sheet and its 58-m sea level equivalent (*1*) is buttressed along most of its periphery by floating extensions of land ice called ice shelves and floating ice tongues (Fig. 1). Ice shelves cover an area >1.561 million km^2, comparable in size to the Greenland Ice Sheet, and fringe 75% of Antarctica's coastline while collecting 20% of its snowfall over 11% of its area (*2*, *3*). These features are nourished by the inflow of continental ice from grounded glaciers, surface accumulation and freezing of marine ice on their undersides. They lose mass to iceberg calving and basal melting along with topside sublimation and wind drift. Ice shelves exert considerable control on glacier stability and Antarctic Ice Sheet mass balance (*4*–*6*) and play significant roles in ocean stratification and bottom water formation (*7*).

The traditional view of ablation from Antarctic ice shelves has been that it occurs mostly by iceberg calving, with basal melting only contributing 10 to 28% of the total mass loss (*3*–*6*). Estimates of ice shelf meltwater production derived from oceanographic data (*8*–*10*, e.g.) are impractical for synoptic circumpolar coverage. Numerical simulations of ice-ocean interactions extend from individual ice shelves to circumpolar models at various resolutions, but comparisons with observations are limited, and estimates of total ice shelf meltwater production have varied from 357 to 1,600 gigatons per year (1 Gt = 10^{12} kg) (*3*, *7*, *11*). Glaciological estimates have focused on few ice shelves (*6*, *12*, *13*) or near a fraction of glacier grounding lines (*14*) due to incomplete velocity and thickness mapping.

Here we present more accurate, higher-resolution glaciological estimates of ice shelf melting around the entire continent. At any point on an ice shelf of thickness H and velocity vector $\mathbf{v}$, the rate of ice shelf thickening $\partial H/\partial t$ equals the sum of net surface mass balance *SMB* minus net basal melting B minus the lateral divergence in volume flux $H\mathbf{v}$ (*15*). A negative value of B indicates the freeze-on of marine ice. The calculation of volume flux divergence on a point per point basis yields the distribution of freeze/melt (Fig. 1). The integration of the total inflow and outflow within the ice shelf perimeters yields the area-average melt rate and total melt water production (Table 1).

For *SMB*, we use output products from the Regional Atmospheric and Climate Model RACMO2 (*16*), which is forced at the lateral boundary and sea surface by global reanalyses of the European Centre for Medium-Range Weather Forecasts. RACMO2 includes surface melt water retention due to refreezing, evaporation, wind drift and sublimation. The products have been validated with field data and an error propagation analysis (*17*) to a precision of 7 to 25%, average 10%, depending on location. We use the average *SMB* for the years 1979–2010 to represent a longer-term state.

Ice shelf thickness is from Operation IceBridge (OIB) (*18*, *19*) and BEDMAP-2 (*1*) (fig. S1, supplementary materials). It combines direct measurements from radio echo sounding, with indirect estimates from altimetry-derived ice shelf surface elevation assuming hydrostatic equilibrium with a nominal precision of 15 to 50 m (*20*). Flux gates are selected at the location of Interferometric Synthetic Aperture Radar (InSAR)–derived grounding lines, which are more precise than derived from photogrammetric techniques or visible imagery (*21*), with accompanying impacts on estimates of volume fluxes. Ice-front flux gates are at the seaward limit of the volume flux data, within 1 to 3 km of ice-front positions digitized from a 150-m spacing mosaic of Advanced Land Observing System (ALOS) Polarimetric SAR (PALSAR) data for the years 2007-2008.

Ice shelf flow vector velocities are from InSAR data collected in 2007–2008 and processed at 450 m spacing (*22*). The average precision in speed is 4 m/year and 1.7° in direction (fig. S2). In the absence of vertical shear on floating ice, the surface-derived velocity is equivalent to a depth-averaged velocity. We survey 99.5% of Antarctic ice shelf area in 2007–2008 (Table 1), or 1.554 million km^2, excluding a few smaller ice shelves where ice thickness is not well known (table S1). Drainage boundaries between ice shelves, including the eastern and western Ross, are defined by flow vector direction. Ice rises and islands are excluded from the ice shelf area estimates but included in the *SMB* calculation.

Ice-shelf thickening $\partial H/\partial t$ for the period 2003–2008 is calculated using the procedure in (*23*), with an error dependent on firn depth corrections (fig. S3). The results are combined with *SMB* and the flux divergence to calculate B, with a precision dominated by uncertainties in ice-front thickness and firn depth corrections (table S1). We also calculate the results for $\partial H/\partial t = 0$, i.e., no ice shelf thickness change, to obtain a reference rate B_{ss} corresponding to the amount of freezing or melting that would be required to maintain an ice shelf in "steady state" for 2007–2008 (fig. S4).

The freeze/melt distribution confirms that basal melting is strongest near the grounding zones of major glaciers and along the ice fronts of some of the largest ice shelves, especially Ronne (Fig. 1). Ice shelf melting decreases away from grounding lines and becomes negative (accretion of marine ice) on all large ice shelves and some smaller ice shelves. This general pattern of melting and freezing beneath ice shelves is well understood (*4*–*6*, *15*) and is governed by the Coriolis-influenced transport and vertical mixing of ocean heat, the pressure-dependence of the freezing point of seawater, and the sea floor and cavity morphology. On some large ice shelves, freezing is concentrated on the western sides, consistent with an oceanic circulation during which seawater is first cooled, freshened and made more buoyant by melting.

The highest melt rates are detected in the southeast Pacific sector of the Antarctic Peninsula and West Antarctica, from the northern end of George VI to the western end of Getz Ice Shelf. On slow-moving to nearly-stationary ice shelves like the Wilkins, George VI, Abbot and Sulzberger, basal melting entirely consumes the inflow of individual glaciers within a few km of their grounding zones. High melt rates are

also revealed in the grounding zones of the Amery, Moscow University, Shackleton, and Totten in East Antarctica.

In contrast, low melt rates are found under the largest ice shelves, e.g., the Ross West, except near deep grounding lines. Maximum grounding line depth is only 0.9 km under the Ross West but 2.1 km under the Filchner and Ronne, 1.8 km under Ross East, and 2.4 km under the Amery (*1*). Each additional 100 m adds 0.076°C to the thermal driving of seawater that may have started out near the sea surface freezing point. Differences in observed melt rate may also be accentuated by variations in flushing time and tidal activity (*24*).

Total ice inflow and outflow for each ice shelf is summarized in Fig. 1 and Table 1. Ice-front flux is a proxy for, but not identical to, iceberg calving, which occurs at irregular time intervals ranging from years to decades. The higher basal melting near some ice-shelf fronts (*12*, *25*) results from stronger tidal currents and mixing, especially in combination with a shallow water column (*24*), as along the eastern front of Ronne [150 ± 50 m in (*1*) versus 350 ± 100 m for Ross or 500 ± 250 m for Filchner]. Ice-front fluxes may overestimate iceberg calving where near ice front melting is significant and calving is infrequent; conversely, large icebergs may on average be thicker than the ice front, in which case ice front fluxes underestimate calving.

The total ice shelf grounding line inflow of 1,696 ± 146 Gt/year combined with an *SMB* input of 430 ± 81 Gt/year is partitioned into an ice-front flux of 1,089 ± 139 Gt/year and a basal meltwater production of 1,325 ± 235 Gt/year. Basal melting thus accounts for 55 ± 10% of ice shelf mass ablation. The corresponding area-average melt rate of 85 ± 15 cm/year is three times as large as the average *SMB* on ice shelves (28 ± 5 cm) and five times the average *SMB* on grounded ice sheet (16 ± 1 cm) (*16*), illustrating the considerable importance of ocean interactions in freshwater transfers between the ice and ocean.

The grounding line flux of all surveyed ice shelves accounts for 83 ± 7% of the total ice discharge into the Southern Ocean (Table 1). Total Antarctic grounded ice discharge (*26*) is 352 ± 30 Gt/year higher than our grounding line flux because of additional discharge from smaller ice shelves and ice walls that terminate in the ocean (*27*). An equal partitioning of these missing areas between calving and basal melting (see supplementary materials) would increase in-situ meltwater production to 1,500 ± 237 Gt/year and ice-front flux to 1,265 ± 139 Gt/year.

The comparison of basal melting, B (Fig. 1) with steady state melting, B_{ss} (fig. S4, Table 1, and table S1) shows that many ice shelves are near equilibrium ($B \sim B_{ss}$), while some are thickening ($B < B_{ss}$) and others are thinning ($B > B_{ss}$). High basal melting is therefore not synonymous with thinning. Ice shelves with high melt rates can be in a state of mass balance, but meltwater production is 28 ± 9% higher than required to maintain the ice shelves in overall steady state (1037 ± 218). Ice shelves in the Amundsen Sea sector (Pine Island to Getz) contribute 59% of the 287 ± 89 Gt/year imbalance, an attrition rate twice that of their glacier source regions over the same time period (*26*). Similarly, the total imbalance of all Antarctic ice shelves combined is more than twice that of the grounded ice (*26*).

The ratio of calving to melting averages 0.45 ± 0.3, but exhibits significant regional variability (Table 1), with area-average melt rates varying from negative to > 40 m/year. This wide range reflects diverse ocean environments, which include seawater temperature, the depths of troughs and sills that influence the access of oceanic heat to ice shelf cavities, and the sea ice formation and drifts resulting from atmospheric forcing.

Large ice shelves generate a disproportionally small portion of the total ice shelf meltwater despite high production rates in their deep grounding zones and along lengthy ice fronts. The four giants with areas > 100,000 km^2 (Ross East, Ross West, Filchner and Ronne) cover 61% of the total ice shelf area but contribute only 15% of the meltwater at an average rate of 13 cm/year. The low melt rates result from the relatively weak ocean heat source provided by cold shelf waters, in turn leading to substantial marine ice accretion (*28*). Despite areas 3-10 times larger than the Getz, none of the big four ice shelves produce as much meltwater, with the Ross West contributing no net melt. Meltwater from the southeast Pacific-Antarctic sector (George VI through Getz) accounts for 48% of the total meltwater over only 8% of the area, with the Getz being the largest meltwater source in Antarctica during the study period. B averages 5.1 m/year in this region, from a maximum of 43 m/year under the short Ferrigno Glacier tongue, to a minimum of 1.8 m/year beneath the Abbot. That area-average rate may seem low for a warm-cavity Southeast Pacific ice shelf, but the moderate-sized, shallow-draft Abbot (*29*) ranks 8th overall in meltwater production, while maintaining a positive mass balance ($B < B_{ss}$).

Meltwater production from several small East Antarctic ice shelves in the Wilkes Land sector is larger than expected. Area-average melt rates from Dibble through Vincennes (4-11 m/year) are comparable to Amundsen Sea ice shelf rates from Crosson through Land (4-11 m/year), while meltwater produced by Shackleton and West (73 and 27 Gt/year) rivals that from Thwaites and Sulzberger (98 and 18 Gt/year). Except for the region from 140-150°W where the Mertz and Ninnis float in cold shelf waters, oceanographic data are sparse along the Wilkes Land coastline. "Modified" warm deep water at a temperature near 0°C has been reported 40 km south of the continental shelf break northeast of Totten (*30*). By analogy with observations in the Amundsen Sea, our results suggest the presence of seawater at similar temperatures under several East Antarctic ice shelves. Even zero-degree seawater at outer continental shelf depths could expose ice shelves with deep grounding lines like the Totten (2.2 km), Moscow (2.0 km) and Shackleton (1.8 km) to temperatures more than 3°C above their melting points. To evaluate the impact of these warm deep waters on ice shelf melting, more information is needed about their spatial and temporal variability on the outer shelf, and links via glacially scoured troughs to the vulnerable glacier grounding lines.

Our glaciological estimates are generally consistent with recent results from high-resolution ocean models in the Amundsen, Bellingshausen, and Weddell Seas (*29*, *31*–*33*) (see supplementary materials), but melting of the largest ice shelves is notably less here than in circumpolar models (*7*, *11*). Discrepancies between model results and observations have been attributed to deficiencies in atmospheric forcing, the representation of sea ice cover, the smoothing of bottom topography and assumptions regarding cavity shape. Some models yield annual cycles and decadal variability (*29*) that can now be compared for specific periods with glaciological measurements, which need to be extended in time.

Our results indicate that basal melting accounts for a larger fraction of Antarctic ice shelf attrition than previously estimated. These improved glaciological estimates not only provide more accurate and detailed reference values for modeling, but a baseline for similar future studies. Ice shelf melt water production exhibits a complex spatial pattern around the continent, with an outsized contribution of smaller, fast-melting ice shelves in both West and East Antarctica. Warm-cavity ice shelves along the southeast Pacific coastline, predicted and observed to be sensitive to ocean warming and circulation strength (*9*, *34*), are thinning and losing mass rapidly. Nearly half of the East Antarctic ice shelves are also thinning, some due to probable exposure to "warm" seawater, with connections to ice drainage basins grounded below sea level.

Continued observations of ice shelf velocity and thickness change, along with more detailed information on cavity shape, seafloor topography and atmospheric and oceanic forcing variability are critical to understand the temporal variability and evolution of Antarctic ice shelves. Continued warming of the ocean will slowly increase ice shelf thinning, but if major shifts in sea ice cover and ocean circulation tip even large ice shelf cavities from cold to warm (*35*), there could be major changes in ice shelf and thus ice sheet mass balance.

References and Notes

1. P. Fretwell *et al*., Bedmap2: Improved ice bed, surface and thickness datasets for Antarctica. *The Cryosphere* **7**, 375 (2013). doi:10.5194/tc-7-375-2013
2. C. W. Swithinbank, *Satellite Image Atlas of Glaciers of the World: Antarctica*, R. S. Williams, J. G. Ferrigno, Eds. (USGS Prof. Paper 1386-B, 1988).
3. N. I. Barkov, *Ice Shelves of Antarctica* (New Delhi, NY, Amerind Pub. Co., 1985).
4. R. LeB. Hooke, *Principles of Glacier Mechanics* (Cambridge University Press, Cambridge, 2005).
5. K. M. Cuffey, W. S. B. Paterson, *The Physics of Glaciers* (Elsevier, Burlington, MA, ed. 4, 2010).
6. S. S. Jacobs, H. H. Hellmer, C. S. M. Doake, A. Jenkins, R. M. Frolich, Melting of ice shelves and the mass balance of Antarctica. *J. Glaciol.* **38**, 375 (1992).
7. H. H. Hellmer, Impact of Antarctic ice shelf basal melting on sea ice and deep ocean properties. *Geophys. Res. Lett.* **31**, L10307 (2004). doi:10.1029/2004GL019506
8. A. Jenkins, S. S. Jacobs, Circulation and melting beneath George VI Ice Shelf, Antarctica. *Geophys. Res. Lett.* **113**, (C4), C04013 (2008). doi:10.1029/2007JC004449
9. S. S. Jacobs, A. Jenkins, C. F. Giulivi, P. Dutrieux, Stronger ocean circulation and increased melting under Pine Island Glacier ice shelf. *Nature Geosc.* **4**, 519 (2011). doi:10.1038/ngeo1188
10. A. Foldvik, T. Gammelsrod, E. Nygaard, S. Osterhus, Current measurements near Ronne Ice Shelf: Implications for circulation and melting. *J. Geophys. Res. Oceans* **106**, (C3), 4463 (2001). doi:10.1029/2000JC000217
11. R. Timmermann, Q. Wang, H. H. Hellmer, Ice-shelf basal melting in a global finite-element sea-ice/ice-shelf/ocean model. *Ann. Glaciol.* **53**, 303 (2012). doi:10.3189/2012AoG60A156
12. I. Joughin, L. Padman, Melting and freezing beneath Filchner-Ronne Ice Shelf, Antarctica. *Geophys. Res. Lett.* **30**, 1477 (2003). doi:10.1029/2003GL016941
13. J. Wen *et al*., Basal melting and freezing under the Amery Ice Shelf, East Antarctica. *J. Glaciol.* **56**, 81 (2010). doi:10.3189/002214310791190820
14. E. Rignot, S. S. Jacobs, Rapid bottom melting widespread near Antarctic Ice Sheet grounding lines. *Science* **296**, 2020 (2002). doi:10.1126/science.1070942 Medline
15. A. Jenkins, C. S. M. Doake, Ice ocean interaction on Ronne Ice Shelf, Antarctica. *J. Geophys. Res.* **96**, (C1), 791 (1991). doi:10.1029/90JC01952
16. J. T. M. Lenaerts *et al*., Modeling drifting snow in Antarctica with a regional climate model: 1. Methods and model evaluation. *J. Geophys. Res.* **117**, (D5), D05108 (2012). doi:10.1029/2011JD016145
17. E. Rignot *et al*., Recent mass loss of the Antarctic Ice Sheet from dynamic thinning. *Nat. Geosci.* **1**, 106 (2008). doi:10.1038/ngeo102
18. C. Allen, IceBridge MCoRDS L2 Ice Thickness. Boulder, Colorado USA: NASA DAAC at the National Snow and Ice Data Center (2010).
19. D. D. Blankenship, S. Kempf, D. Young, IceBridge HiCARS 2 L2 Geolocated Ice Thickness. Boulder, Colorado USA: NASA DAAC at the National Snow and Ice Data Center (2012).
20. J. A. Griggs, J. L. Bamber, Antarctic ice-shelf thickness from satellite radar altimetry. *J. Glaciol.* **57**, 485 (2011). doi:10.3189/002214311796905659
21. E. Rignot, J. Mouginot, B. Scheuchl, Antarctic grounding line mapping from differential satellite radar interferometry. *Geophys. Res. Lett.* **38**, L10504 (2011). doi:10.1029/2011GL047109
22. E. Rignot, J. Mouginot, B. Scheuchl, Ice flow of the Antarctic ice sheet. *Science* **333**, 1427 (2011). doi:10.1126/science.1208336 Medline
23. H. D. Pritchard *et al*., Antarctic ice-sheet loss driven by basal melting of ice shelves. *Nature* **484**, 502 (2012). doi:10.1038/nature10968 Medline
24. K. Makinson, P. R. Holland, A. Jenkins, K. Nicholls, D. M. Holland, Influence of tides on melting and freezing beneath Filchner Ronne Ice Shelf, Antarctica. *Geophys. Res. Lett.* **38**, L06601 (2011). doi:10.1029/2010GL046462
25. H. J. Horgan, R. T. Walker, S. Anandakrishnan, R. B. Alley, Surface elevation changes at the front of the Ross Ice Shelf: Implications for basal melting. *J. Geophys. Res.* **116**, (C2), C02005 (2011). doi:10.1029/2010JC006192
26. A. Shepherd *et al*., A reconciled estimate of ice-sheet mass balance. *Science* **338**, 1183 (2012). doi:10.1126/science.1228102 Medline
27. S. Neshyba, E. G. Josberger, On the estimation of Antarctic iceberg melt rate. *J. Phys. Oceanogr.* **10**, 1681 (1980). doi:10.1175/1520-0485(1980)010<1681:OTEOAI>2.0.CO;2
28. K. Grosfeld *et al*., Marine ice beneath Filchner Ice Shelf: Evidence from a multi-disciplinary approach. *Antarct. Res. Ser.* **75**, 319 (1998). doi:10.1029/AR075p0319
29. M. P. Schodlok, D. Menemenlis, E. Rignot, M. Studinger, Sensitivity of the ice shelf ocean system to the sub-ice shelf cavity shape measured by NASA IceBridge in Pine Island Glacier, West Antarctica. *Ann. Glaciol.* **53**, 156 (2012). doi:10.3189/2012AoG60A073
30. G. D. Williams *et al*., Late winter oceanography off the Sabrina and BANZARE coast (117–1281°E), East Antarctica. *Deep Sea Res. Part II Top. Stud. Oceanogr.* **58**, 1194 (2011). doi:10.1016/j.dsr2.2010.10.035
31. P. R. Holland, A. Jenkins, D. Holland, Ice and ocean processes in the Bellingshausen Sea, Antarctica. *Geophys. Res. Lett.* **115**, (C5), C05020 (2010). doi:10.1029/2008JC005219
32. L. Padman *et al*., Oceanic controls on the mass balance of Wilkins Ice Shelf, Antarctica. *J. Geophys. Res.* **117**, (C1), C01010 (2012). doi:10.1029/2011JC007301
33. P. R. Holland, H. F. J. Corr, D. G. Vaughan, A. Jenkins, P. Skvarca, Marine ice in Larsen Ice Shelf. *Geophys. Res. Lett.* **36**, L11604 (2009). doi:10.1029/2009GL038162
34. P. R. Holland, A. Jenkins, D. M. Holland, The response of ice shelf basal melting to variations in ocean temperature. *J. Clim.* **21**, 2558 (2008). doi:10.1175/2007JCLI1909.1
35. H. H. Hellmer, F. Kauker, R. Timmermann, J. Determann, J. Rae, Twenty-first-century warming of a large Antarctic ice-shelf cavity by a redirected coastal current. *Nature* **485**, 225 (2012). doi:10.1038/nature11064 Medline
36. T. A. Scambos, T. M. Haran, M. A. Fahnestock, T. H. Painter, J. Bohlander, MODIS-based Mosaic of Antarctica (MOA) data sets: Continent-wide surface morphology and snow grain size. *Remote Sens. Environ.* **111**, 242 (2007). doi:10.1016/j.rse.2006.12.020
37. R. A. Bindschadler *et al*., Getting around Antarctica: New high-resolution mappings of the grounded and freely-floating boundaries of the Antarctic Ice Sheet created for the International Polar Year. *The Cryosphere* **5**, 569 (2011). doi:10.5194/tc-5-569-2011
38. J. Mouginot, B. Scheuchl, E. Rignot, Mapping of ice motion in Antarctica using synthetic-aperture radar data. *Remote Sens.* **4**, 2753 (2012). doi:10.3390/rs4092753
39. R. J. Motyka, L. Hunter, K. A. Echelmeyer, C. Connor, Submarine melting at the terminus of a temperate tide-water glacier, LeConte Glacier, Alaska. *Ann. Glaciol.* **36**, 57 (2003). doi:10.3189/172756403781816374
40. E. Rignot, M. Koppes, I. Velicogna, Rapid submarine melting of the calving faces of west Greenland glaciers. *Nat. Geosci.* **3**, 187 (2010). doi:10.1038/ngeo765
41. A. J. Fox, A. Paul, R. Cooper, Measured properties of the Antarctic Ice Sheet derived from the SCAR Antarctic digital database. *Polar Rec. (Gr. Brit.)* **30**, 201 (1994). doi:10.1017/S0032247400024268
42. A. J. Cook, D. G. Vaughan, Overview of areal changes of the ice shelves on the Antarctic Peninsula over the past 50 years. *The Cryosphere* **4**, 77 (2010). doi:10.5194/tc-4-77-2010
43. T. Gammelsrød *et al*., Distribution of water masses on the continental shelf in the southern Weddell Sea, in *The Polar Oceans and Their Role in Shaping the Global Environment, Geophys. Monogr. Ser.*, vol. 85, O. M. Johannessen, R. D. Muench, J. E. Overland (Eds.), pp. 159–176 (AGU, Washington, D. C., 1994), pp.

159–176; doi:10.1029/GM085p0159.
44. P. Schlosser *et al*., Oxygen 18 and helium as tracers of ice shelf water and water/ice interaction in the Weddell Sea. *J. Geophys. Res.* **95**, (C3), 3253 (1990). doi:10.1029/JC095iC03p03253
45. A. S. Shepherd *et al*., Recent loss of floating ice and the consequent sea level contribution. *Geophys. Res. Lett.* **37**, L13503 (2010). doi:10.1029/2010GL042496
46. R. H. Thomas *et al*., A comparison of Greenland ice-sheet volume changes derived from altimetry measurements. *J. Glaciol.* **54**, 203 (2008). doi:10.3189/002214308784886225
47. E. J. Rignot, Fast recession of a west Antarctic glacier. *Science* **281**, 549 (1998). doi:10.1126/science.281.5376.549 Medline
48. A. J. Payne *et al*., Numerical modeling of ocean-ice interactions under Pine Island Bay's ice shelf. *J. Geophys. Res.* **112**, (C10), C10019 (2007). doi:10.1029/2006JC003733
49. C. S. M. Doake, Glaciological Evidence: Antarctic Peninsula, Weddell Sea; *Glaciers, Ice Sheets, and Sea Level: Effect of a CO2-induced Climatic Change*, Seattle Workshop, Washington, 13-15 Sep 1984, USDOE/ER/60235-1, 197-209, (1985)
50. S. S. Jacobs, H. H. Hellmer, A. Jenkins, Antarctic ice sheet melting in the southeast Pacific. *Geophys. Res. Lett.* **23**, 957 (1996). doi:10.1029/96GL00723
51. R. Gerdes, J. Determann, K. Grosfeld, Ocean circulation beneath Filchner-Ronne Ice Shelf from three-dimensional model results. *J. Geophys. Res.* **104**, (C7), 15,827 (1999). doi:10.1029/1999JC900053
52. K. W. Nicholls *et al*., Water mass modification over the continental shelf north of Ronne Ice Shelf, Antarctica. *J. Geophys. Res.* **108**, (C8), 3260 (2003). doi:10.1029/2002JC001713
53. A. Jenkins, D. G. Vaughan, S. S. Jacobs, H. H. Hellmer, J. R. Keys, Glaciological and oceanographic evidence of high melt rates beneath Pine Island Glacier, West Antarctica. *J. Glaciol.* **43**, 114 (1997).
54. H. H. Hellmer, S. S. Jacobs, A. Jenkins, Oceanic erosion of a floating Antarctic glacier in the Amundsen Sea. *Antarct. Res. Ser.* **75**, 83 (1998). doi:10.1029/AR075p0083
55. A. Shepherd, D. Wingham, E. Rignot, Warm ocean is eroding West Antarctic Ice Sheet. *Geophys. Res. Lett.* **31**, L23402 (2004). doi:10.1029/2004GL021106
56. R. A. Bindschadler, D. G. Vaughan, P. Vornberger, Variability of basal melt beneath the Pine Island Glacier ice shelf, West Antarctica. *J. Glaciol.* **57**, 581 (2011). doi:10.3189/002214311797409802
57. P. Heimbach, M. Losch, Adjoint sensitivities of sub-ice-shelf melt rates to ocean circulation under the Pine Island Ice Shelf, West Antarctica. *Ann. Glaciol.* **53**, 59 (2012). doi:10.3189/2012/AoG60A025
58. T. Hughes, The Stability of the West Antarctic Ice Sheet: What has happened and what will happen, *Proceedings, Carbon Dioxide Research Conference: CO2, Science and Consensus*, Berkeley Springs Workshop, 19-23 Sep 1982, USDOE, 820970-021, DE-AC05-76OR00033, 021, IV.62 (1983).

Acknowledgments: We thank three anonymous reviewers for their constructive criticism of the manuscript. This work was performed at the University of California Irvine and at the Jet Propulsion Laboratory, California Institute of Technology under grants from NASA's Cryospheric Science Program and Operation IceBridge (OIB), and at the Lamont-Doherty Earth Observatory of Columbia University under grants from the National Science Foundation and the National Oceanic and Atmospheric Administration.

Supplementary Materials
www.sciencemag.org/cgi/content/full/science.1235798/DC1
Supplementary Text
Figs. S1 to S4
Tables S1 and S2
References (*36–58*)

29 January 2013; accepted 31 May 2013
Published online 13 June 2013
10.1126/science.1235798

Table 1. Meltwater production of Antarctic ice shelves, with ice shelves named counter clockwise in Fig. 1. Areas in square kilometers exclude ice rises and islands. Grounding line flux (GL), surface mass balance (SMB), ice-front (proxy for calving) flux (Ice Front), ice-shelf mass gain ($\partial H/\partial t$ in water mass equivalent), and basal meltwater production in gigatons (1 Gt = 10^{12} kg) per year, with area-average basal melt rate in meter of water per year indicated in parenthesis. Total Antarctica on the last row includes non-surveyed coastal sectors. Ice shelf names are from United States Geological Survey and (3). Surveyed ice-shelf mass loss of 287 ± 89 Gt/year in 2003–2008 ($\partial H/\partial t$) is 28 ± 9% higher than that required to maintain the ice shelves in steady state for 2003–2008. *, Larsen B data (velocity, thickness) prior to the 2002 collapse; thinning rate from the remnant part of the ice shelf only. Additional details in table S1.

Name	Area km^2	GL Gt/year	SMB Gt/year	Ice front Gt/year	$\partial H/\partial t$ Gt/year	Basal melt Gt/year (m/year)
Larsen G	412	0.9 ± 0.2	0.1 ± 0	0.7 ± 1	0.0 ± 0	0.3 ± 0.2 (0.71 ± 0.6)
Larsen F	828	1.5 ± 0.3	0.3 ± 0.1	0.6 ± 1	-0.7 ± 0.5	1.2 ± 0.4 (1.4 ± 0.5)
Larsen E	1,184	3.6 ± 0.7	0.4 ± 0.1	1.5 ± 1	1.1 ± 0.7	1.4 ± 1 (1.2 ± 0.9)
Larsen D	22,548	18.5 ± 4	9.8 ± 2	6.3 ± 1	20.5 ± 14	1.4 ± 14 (0.1 ± 0.6)
Larsen C	46,465	29.6 ± 3	23.8 ± 4	31.3 ± 3	1.4 ± 67	20.7 ± 67 (0.4 ± 1)
Larsen B*	6,755	13.6 ± 3	3.0 ± 0.6	8.9 ± 1	-4.5 ± 13	12.2 ± 14 (1.8 ± 2)
Wordie	277	13.8 ± 1	0.3 ± 0	7.6 ± 3	-0.1 ± 0	6.5 ± 3 (23.6 ± 10)
Wilkins	12,866	7.8 ± 2	8.3 ± 2	0.7 ± 0.4	-3.4 ± 16	18.4 ± 17 (1.5 ± 1)
Bach	4,579	5.4 ± 1	1.8 ± 0.3	0.8 ± 0.2	-4.0 ± 0.3	10.4 ± 1 (2.3 ± 0.3)
George VI	23,434	68.2 ± 5	12.7 ± 2	5.7 ± 1.2	-13.8 ± 16	89.0 ± 17 (3.8 ± 0.7)
Stange	8,027	21.0 ± 3	6.0 ± 1	4.6 ± 0.8	-5.6 ± 5	28.0 ± 6 (3.5 ± 0.7)
Ant. Peninsula	127,375	184 ± 26	66 ±13	69 ± 13	-9 ± 74	191 ± 80 (1.5 ± 0.6)
Ronne	338,887	156.1 ± 10	59.3 ± 11	149.2 ± 22	-47.4 ± 22	113.5 ± 35 (0.3 ± 0.1)
Ferrigno	117	11.2 ± 1	0.16 ± 0	6.6 ± 2	-0.3 ± 0	5.1 ± 2 (43.4 ± 17)
Venable	3,194	14.6 ± 2	3.5 ± 1	6.5 ± 1	-7.7 ± 1	19.4 ± 2 (6.1 ± 0.7)
Abbot	29,688	34.0 ± 4	25.0 ± 5	2.4 ± 0.5	4.7 ± 18	51.8 ± 19 (1.7 ± 0.6)
Cosgrove	3,033	5.2 ± 1	1.5 ± 0.3	1.3 ± 1.2	-3.1 ± 2	8.5 ± 2 (2.8 ± 0.7)
Pine Island	6,249	126.4 ± 6	4.6 ± 0.9	62.3 ± 5	-33.2 ± 2	101.2 ± 8 (16.2 ± 1)
Thwaites	5,499	113.5 ± 4	4.8 ± 0.9	54.5 ± 5	-33.7 ± 3	97.5 ± 7 (17.7 ± 1)
Crosson	3,229	27.4 ± 2	3.7 ± 0.7	11.7 ± 2	-19.2 ± 1	38.5 ± 4 (11.9 ± 1)
Dotson	5,803	28.4 ± 3	5.7 ± 1	5.5 ± 0.7	-16.6 ± 2	45.2 ± 4 (7.8 ± 0.6)
Getz	34,018	96.7 ± 5	34.2 ± 7	53.5 ± 2	-67.6 ± 12	144.9 ± 14 (4.3 ± 0.4)
Land	640	14.5 ± 1	0.8 ± 0.1	12.2 ± 1	-0.7 ± 0.3	3.8 ± 1 (5.9 ± 2)
Nickerson	6,495	7.8 ± 1	4.6 ± 0.9	4.3 ± 0.6	3.9 ± 1	4.2 ± 2 (0.6 ± 0.3)
Sulzberger	12,333	15.1 ± 2	8.2 ± 2	1.0 ± 0.2	4.1 ± 2	18.2 ± 3 (1.5 ± 0.3)
Swinburne	900	4.9 ± 0.4	0.9 ± 0.2	1.5 ± 0.3	0.6 ± 0.2	3.8 ± 0.5 (4.2 ± 0.6)
Withrow	632	1.3 ±0.2	0.3 ± 0.0	1.2 ± 0.3	0.1 ± 0.1	0.3 ± 0.4 (0.5 ± 0.6)
Ross West	306,105	73.0 ± 4	33.5 ± 6	100.4 ± 8	7.6 ± 17	-1.4 ± 20 (0.0 ± 0.1)
West Antarctica	756,822	730 ± 47	191 ± 36	494 ± 57	-208 ± 36	654 ± 89 (0.9 ± 0.1)
Ross East	194,704	56.1 ± 4	31.0 ± 6	45.9 ± 4	-7.8 ± 11	49.1 ± 14 (0.3 ± 0.1)
Drygalski	2,338	9.6 ± 0.6	0.3 ± 0.1	3.0 ± 1	-0.8 ± 0.4	7.6 ± 1 (3.3 ± 0.5)
Nansen	1,985	1.3 ± 0.5	0.3 ± 0.1	0.2 ± 0.1	0.4 ± 0.1	1.1 ± 0.6 (0.6 ± 0.3)
Aviator	785	1.1 ± 0.2	0.2 ± 0.	0.2 ± 0.1	-0.3 ± 0.1	1.4 ± 0.2 (1.7 ± 0.3)
Mariner	2,705	2.5 ± 0.4	1.1 ± 0.2	0.6 ± 0.2	0.6 ± 0.3	2.4 ± 0.6 (0.9 ± 0.2)
Lillie	770	3.6 ± 0.3	0.2 ± 0.	0.5 ± 0.1	0.0 ± 0.	3.4 ± 0.3 (4.4 ± 0.4)
Rennick	3,273	4.8 ± 1	0.7 ± 0.1	0.8 ± 0.2	-2.3 ± 0.9	7.0 ± 1 (2.2 ± 0.3)
Cook	3,462	36.0 ± 3	1.7 ± 0.3	27.6 ± 3	5.5 ± 1	4.6 ± 5 (1.3 ± 1)
Ninnis	1,899	27.6 ±2	1.3 ± 0.2	24.6 ± 3	2.0 ± 0.9	2.2 ± 3 (1.2 ± 2)
Mertz	5,522	20.0 ± 1	3.6 ± 0.7	12.0 ± 2	3.6 ± 1	7.9 ± 3 (1.4 ± 0.6)
Dibble	1,482	12.5 ± 1	1.5 ± 0.3	8.2 ± 0.9	-2.3 ± 0.7	8.1 ± 1 (5.5 ± 0.9)
Holmes	1,921	26.0 ± 2	2.8 ± 0.5	24.7 ± 4	-2.5 ± 1	6.7 ± 4 (3.5 ± 2)
Moscow Univ.	5,798	52.3 ± 1	4.7 ± 0.9	29.6 ± 3	-0.1 ± 3	27.4 ± 4 (4.7 ± 0.8)
Totten	6,032	71.0 ± 3	6.2 ± 1	28.0 ± 2	-14.0 ± 2	63.2 ± 4 (10.5 ± 0.7)
Vincennes	935	12.7 ± 1	0.5 ± 0.1	6.8 ± 1	1.3 ± 0.6	5.0 ± 2 (5.3 ± 2)
Conger/Glenzer	1,547	1.7 ± 0.4	0.9 ± 0.2	1.1 ± 0.8	-2.1 ± 1	3.6 ± 1 (2.3 ± 0.9)
Tracy/Tremenchus	2,845	0.6 ±0.4	1.0 ± 0.2	0.2 ± 0.1	-1.7 ± 2	3.0 ± 2 (1.5 ± 0.7)
Shackleton	26,080	55.0 ± 4	16.2 ± 3	30.3 ± 3	-31.7 ± 14	72.6 ± 15 (2.8 ± 0.6)
West	15,666	41.9 ± 4	6.9 ± 1	32.6 ± 7	-11.1 ± 7	27.2 ± 10 (1.7 ± 0.7)
Publications	1,551	5.8 ± 0.8	0.4 ± 0.1	5.2 ± 1	-0.5 ± 0.8	1.5 ± 2 (1.0 ± 1)
Amery	60,654	56.0 ± 0.5	8.5 ± 2	50.4 ± 8	-21.4 ± 21	35.5 ± 23 (0.6 ± 0.4)
Wilma/Robert/Downer	858	10.3 ±0.5	0.6 ± 0.1	0.8 ± 0.4	0.0 ± 0	10.0 ± 0.6 (11.7 ± 0.7)
Edward VIII	411	4.1 ± 0.8	0.4 ± 0.1	0.3 ± 0.1	0.0 ± 0	4.2 ± 0.8 (10.2 ± 2)
Rayner/Thyer	641	14.2 ± 1	0.3 ± 0.1	7.8 ± 0.6	0.0 ± 0	6.7 ± 1 (10.5 ± 2)
Shirase	821	15.0 ± 1	0.4 ± 0.1	9.6 ± 1	0.0 ± 0	5.7 ± 1 (7.0 ± 2)
Prince Harald	5,392	8.3 ± 1	4.1 ± 0.8	10.3 ± 2	4.0 ± 2	-2.0 ± 3 (-0.4 ± 0.6)
Baudouin	32,952	22.0 ± 3	8.4 ± 2	6.5 ± 1	9.8 ± 11	14.1 ± 12 (0.4 ± 0.4)
Borchgrevink	21,580	19.6 ± 3	6.1 ± 1	17.5 ± 3	0.7 ± 4	7.5 ± 6 (0.3 ± 0.3)
Lazarev	8,519	3.7 ± 0.6	2.0 ± 0.4	3.1 ± 1	-3.6 ± 2	6.3 ± 2 (0.7 ± 0.2)
Nivl	7,285	3.9 ± 0.8	1.8 ± 0.3	1.3 ± 0.4	0.6 ± 1	3.9 ± 2 (0.5 ± 0.2)
Vigrid	2.089	2.7 ± 0.4	0.4 ± 0.1	2.0 ± 0.4	-2.0 ± 0.4	3.2 ± 0.7 (1.5 ± 0.3)
Fimbul	40,843	24.9 ± 4	12.7 ± 2	18.2 ± 2	-4.0 ± 7	23.5 ± 9 (0.6 ± 0.2)
Jelbart	10,844	9.9 ± 1	4.9 ± 0.9	8.8 ± 2	6.9 ± 2	-1.0 ± 3 (-0.1 ± 0.3)
Atka	1,969	0.9 ± 0.2	0.8 ± 0.1	1.0 ± 0.2	1.1 ± 0.2	-0.5 ± 0.4 (-0.2 ± 0.2)
Ekstrom	6,872	4.1 ± 0.8	2.6 ± 0.5	2.3 ± 0.6	0.0 ± 0	4.3 ± 2 (0.6 ± 0.2)
Quar	2,156	1.0 ±0.2	0.5 ± 0.1	0.6 ± 0.1	-0.5 ± 0.4	1.4 ± 0.5 (0.7 ± 0.2)
Riiser-Larsen	43,450	21.5 ± 3	12.7 ± 2	12.1 ± 2	13.4 ± 8	8.7 ± 9 (0.2 ± 0.2)
Brunt/Stancomb	36,894	20.3 ± 3	11.4 ± 2	28.1 ± 4	2.6 ± 4	1.0 ± 7 (0.03 ± 0.2)
Filchner	104,253	97.7 ± 6	13.4 ± 2	82.8 ± 4	-13.6 ± 7	41.9 ± 10 (0.4 ± 0.1)
East Antarctica	669,781	782 ± 80	174 ± 33	546 ± 70	-70 ± 34	480 ± 116 (0.7 ± 0.2)
Total surveyed	**1,553,978**	**1,696 ± 146**	**430 ± 81**	**1,089 ± 139**	**-287 ± 89**	**1,325 ± 235 (0.85 ± 0.1)**
Total Antarctica	1,561,402	2,048 ± 149		1,265 ± 141		1,500 ± 237

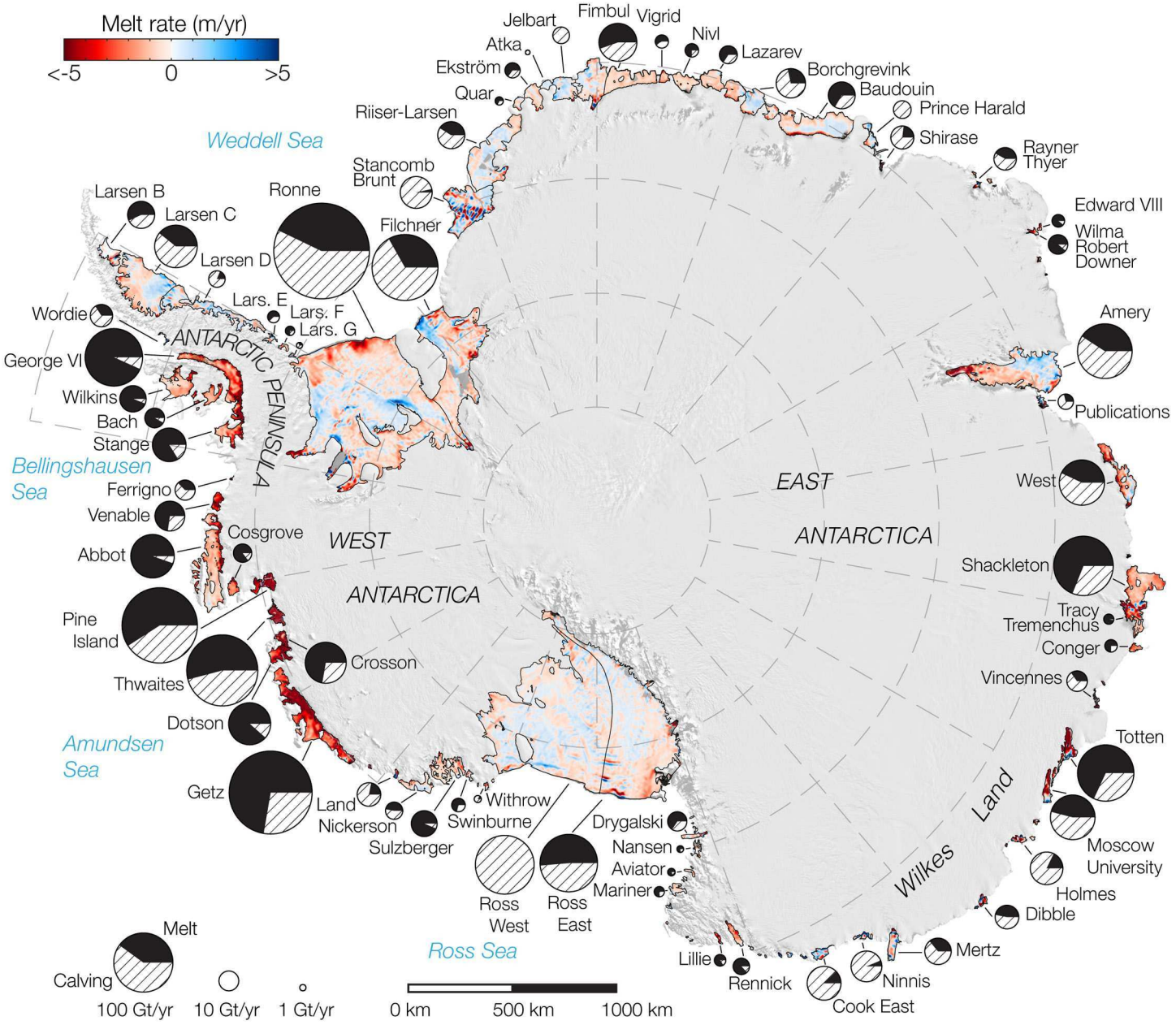

Fig. 1. Basal melt rates of Antarctic ice shelves color coded from < –5 m/year (freezing) to > +5 m/year (melting) and overlaid on a 2009 MODIS mosaic of Antarctica. Ice-shelf perimeters in 2007–2008, excluding ice rises and ice islands, are thin black lines. Each circle graph is proportional in area to the mass loss from each shelf, in gigatons (1 Gt = 10^{12} kg) per year, partitioned between iceberg calving (hatch fill) and basal melting (black fill). See Table 1 and table S1 for additional details on ice shelf locations, areas, and mass balance components.

www.sciencemag.org/cgi/content/full/science.1235798/DC1

Supplementary Materials for

Ice Shelf Melting Around Antarctica

E. Rignot,* S. Jacobs, J. Mouginot, B. Scheuchl

*Corresponding author. E-mail: erignot@uci.edu

Published 13 June 2013 on *Science* Express
DOI: 10.1126/science.1235798

This PDF file includes:

Other Supplementary Material for this manuscript includes the following:
(available at www.sciencemag.org/cgi/content/full/science.1235798/DC1)

Table S1 (Excel file)

Supplementary Text

Contents

§1. Ice shelf thickness

Ice thickness (Fig. S1) is from BEDMAP-2 *(1)* and NASA Operation IceBridge (OIB) *(18-19*), which are available, respectively, at www.antarctica.ac.uk › Projects AZ › Bedmap2 and at the National Snow and Ice Data Center nsidc.org/data/icebridge/data_summaries.html. BEDMAP-2 merges measurements of ice thickness from airborne radio echo sounding with estimates derived from radar-altimetry observations of surface elevation from 1994 *(20)*. The altimetry product uses the most inland grounding line positions from InSAR *(21),* MOA *(36)* or ASAID *(37)* to minimize the omission of floating sectors. Ice thickness may be erroneously high where ice is not in hydrostatic equilibrium, e.g. in a transition region. Along most glaciers, MOA and ASAID grounding lines (GL) have lateral errors up to 50 km *(21),* which impact the calculation of ice thickness, volume flux and basal melt rate. Here, we only rely a systematic, precise mapping of GL with InSAR (available at nsidc.org/data/docs/measures/nsidc0498_rignot/), and minimize the risk of including grounded ice sectors.

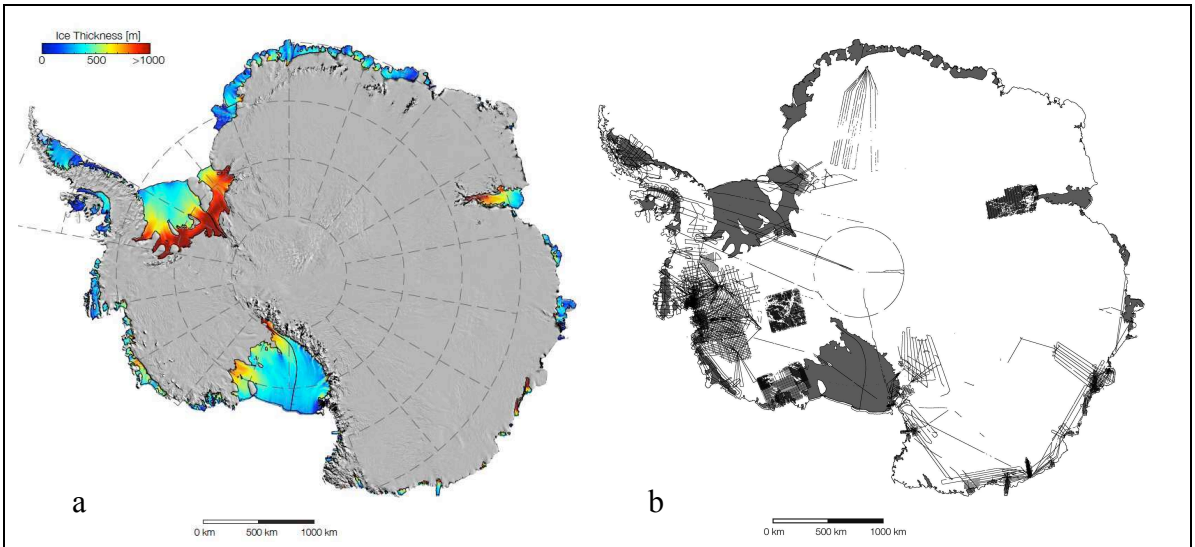

Figure S1. Ice shelf thickness from a) BEDMAP-2 *(1)* with b) flight tracks of NASA OIB and (historical) National Science Foundation (NSF) missions. Ice is thickest near grounding zones and thinnest near ice fronts. Glacier mass inputs are traceable along ice shelves as areas of thicker ice aligned with the flow direction.

Special cases: As GL ice thickness is not well known on Larsen D-G, we use balance discharge from RACMO2 for the GL flux (Table S1). At the GL of Larsen C, Rayner/Thyer, Edward VIII and the thickest parts of Shackleton (Denman Glacier) and Moscow University Ice Shelves, ice thickness assumes hydrostatic equilibrium. For Larsen B, we use ice velocity from 2000 and ice-shelf thickness from 1994 - pre-dating its 2002 collapse. For the GL of Ross East, Nansen, Aviator, Mariner, Ninnis, Mertz, Dibble, Holmes, Totten, Wilma/Robert/Downer, Rayner/Thyer and Shirase in East Antarctica (EAIS), and Land, Nickerson, Sulzberger and Swinburne in West Antarctica (WAIS), we use *(20)*; for David Glacier, we use OIB. For ice-front fluxes, we use BEDMAP-2, except for Rayner/Thyer where ice thickness uses hydrostatic equilibrium.

§2. Ice shelf velocity

Ice-shelf vector velocity data is from a mosaic of InSAR data from six sensors *(22)*. Figure S2 shows the distribution of errors in a) speed and b) flow direction over the study area as discussed in *(38)*. Flow speeds are highest along the coast and on ice shelves. The error in speed is lowest in fast-moving areas mapped with multiple sensors and highest in slow-moving areas mapped using only Advanced Land Observing System (ALOS) Polarimetric Advanced L-band Synthetic Aperture Radar (PALSAR) data. The average errors in flow speed and direction are, respectively, 4 m/yr and 1.7°. The velocity data are available online at nsidc.org/data/docs/measures/nsidc0484_rignot.

a b

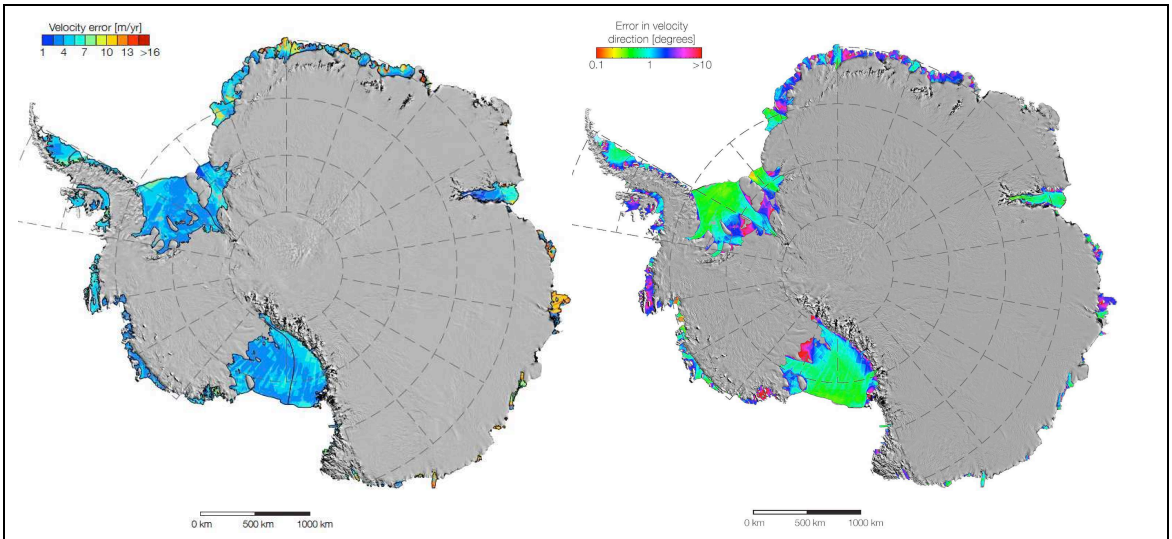

Figure S2. Error in a) velocity magnitude and b) flow direction in 2007-2008 on Antarctic ice shelves, overlaid on a 2009 MODIS mosaic of Antarctica updated from *(36)*. Color coding is linear for speed and logarithmic for direction.

§3. Drainage boundaries

Drainage boundaries on continental ice are traditionally drawn using a digital elevation model of the ice sheet, assuming steady-state ice flow along the lines of steepest surface slope. This approach is not reliable on ice shelves due to their small surface slope. We use flow vector direction to delineate drainage boundaries between adjacent ice shelves. This approach helps to differentiate the ice flow into Filchner Ice Shelf (East Antarctica Ice Sheet (EAIS)) from Academy Glacier (not shown in Fig.~1) versus ice flow into Ronne Ice Shelf (West Antarctica Ice Sheet (WAIS)) from Foundation Ice Stream (not shown in Figure 1). We also separate ice flow into Ross West (WAIS) versus Ross East (EAIS) and ice flow into Brunt-Stancomb versus Riiser-Larsen ice shelves. The transition between EAIS and WAIS is thus defined at the boundaries between Foundation Ice Stream and Academy Glacier in the Weddell Sea sector, and Mercer Ice Stream and Scott Glacier (glaciers not shown in Fig. 1 and Table 1) in the Ross Sea sector.

§4. Ice-front positions

We identify ice-front positions in a radar mosaic of ALOS PALSAR data for the years 2007-2008 at a 150-m posting. The results are compared for consistency and quality control with MOA 2009 updated from *(36)*. As an ice front migrates with ice flow and calving events, an exact agreement is not expected, but the comparison helps identify and resolve discrepancies. In the case of broken ice shelves, where icebergs are partially detached and glued together with an ice mélange of iceberg debris, sea ice and blown snow, ice front delineation uses clues from both radar and visible imagery.

The 2007-2008 ice-front positions do not coincide with the boundaries of BEDMAP-2 because the data sets are from slightly different time periods. As a result, our ice front flux gates are slightly upstream of the 2007-2008 ice front positions. The area in between the ice-front flux gates and the actual ice front positions is 2% of the total ice shelf area.

For ice walls and smaller ice shelves excluded from our survey, we assume a 50/50 partitioning between calving and basal melt to balance the incoming flux, as in the case of tidewater glaciers *(39-40)* (most listed below Table S1).

§5. Ice shelf areas, rises and islands

Inflow from ice rises ice islands along the ice shelf perimeter is included in the GL flux. Ice rises, rumples and islands within the ice shelf perimeters are included in the *SMB* input but excluded from the ice shelf area used to calculate total melt water production.

In Table 1 (and Table S1), we list the survey area of each ice shelf based on the locations of GL and ice-front flux gates. The survey area is used to calculate the melt rate in meters per year. Total melt water production is then obtained by multiplying this melt rate by the actual ice shelf area. Shape files of actual ice shelf perimeters used in this study will be made available at NSIDC under the Antarctic MEaSUREs project.

§6. Grounding line fluxes.

We have compared our GL fluxes with the balance fluxes calculated using RACMO2 *(16)*. GL fluxes are within error bars of the balance fluxes except in a few areas known to be thinning rapidly *(23)*. This verification provides an evaluation of the quality of the thickness data at the grounding line and helps justify the selection of alternative ice thickness estimates, as per the discussion in section 1, “Special cases”.

§7. Surface mass balance (SMB)

We employ SMB products from the University of Utrecht’s Regional Atmospheric Climate Model (RACMO2) validated with in-situ data *(16)*. An error rate has been quantified for each basin based on error propagation *(17)*, which we use in Table S1. We use an average *SMB* for the time period 1979-2010 to obtain a long-term average SMB. Employing *SMB* values for 2007-2008, the time period of velocity mapping, would

introduce significant noise and assume that ice shelf velocities respond instantaneously to annual fluctuations in snow input.

§8. Basal melt rates

The actual basal melt rate, B, in meters per year is deduced from the equation of mass conservation *(15):* $\partial H/\partial t = SMB - B - \nabla (H \boldsymbol{v})$, where H is the ice thickness, $\boldsymbol{v}$ is the ice velocity vector, SMB the surface mass balance, and $\partial H/\partial t$ the rate of ice shelf thickening (positive for ice shelf growth).

To take into account the spatial resolution of the thickness data, we calculate the derivative terms of the mass conservation equation with a 10-km baseline, and the final melt rate map is smoothed with a 10-km filter. As a result, we miss points along the ice shelf perimeters when mapping the freeze/melt distribution; but this does not affect the estimation of area-average melt rates (B expressed in Gt/yr in Table 1 and S1) because that calculation is based on the total inflow and outflow within the ice shelf perimeters, not the integration of point values.

We also calculate melt rates B_{ss} for $\partial H/\partial t = 0$, i.e. the amount of freezing and melting that would be required to maintain the ice shelves in a steady state of velocity and thickness in 2007-2008. For this calculation, we still use velocity data for 2007-2008. In reality, some of these glaciers have been accelerating in recent decades, e.g. several glaciers draining into the Amundsen Sea. For these glaciers, it would have been preferable to use ice velocities from an earlier time period, e.g. 1975, when the system seemed closer to steady state. As we do not have complete velocity and thickness data for that time period, we focus instead on the most complete data set.

The spatial pattern of the melt rate B appears noisy on some ice shelves, in particular on Brunt-Stancomb or Ross. Part of this signal is real and associated with rifts, cracks and vertical undulations in surface elevation present on those shelves. Part of the signal is caused by the time difference between ice thickness and ice velocity data and the advection of heterogeneities in ice thickness along flow. Furthermore, basal melting is expected to be non-uniform across such zones, with melting dominant along the rift sides and freezing dominant at the rift center.

We first calculate the basal melt rates in meters per year over the surveyed areas from the GL flux, ice front flux, SMB and $\partial H/\partial t$. The result is then applied to the actual ice shelf area to deduce the total ice shelf melt water production. We then re-calculate SMB and $\partial H/\partial t$ over the actual ice shelf areas instead of the surveyed area; the grounding line fluxes are unchanged because surveyed and actual areas share identical GL positions. The ice front fluxes are however corrected for the adjustment in SMB and $\partial H/\partial t$ to insure closure of the mass balance equation. This correction amounts to 30 Gt/yr, i.e., < 3% of the total ice front flux, which covers 99.5% of the Antarctic ice shelf area.

§9. Adjustments for ice shelf thickening

Ice shelf thickening $\partial H/\partial t$ is derived using corrected ICESat-1 altimetry data for the period 2003-2008, and surface mass balance and firn correction data posted at dx.doi.org/10.1594/PANGAEA.775984. The analysis follows the method in *(23).* Firn depth corrections provided for 100 ice shelves are interpolated to all ice shelves using inverse distance weighting. The results (Fig. S3) are combined with the flux divergence and *SMB* data to calculate the melt rate *B*. The uncertainty in ice shelf thickening listed in Table S1 is from *(23).* Our results are consistent with *(23).*

Early in 2013, the National Snow and Ice Data Center reported an error of omission in the processing of ICESat data that introduces a 5-10 cm error on a pulse-by-pulse basis. Application of inter-campaign corrections and averaging over the entire time

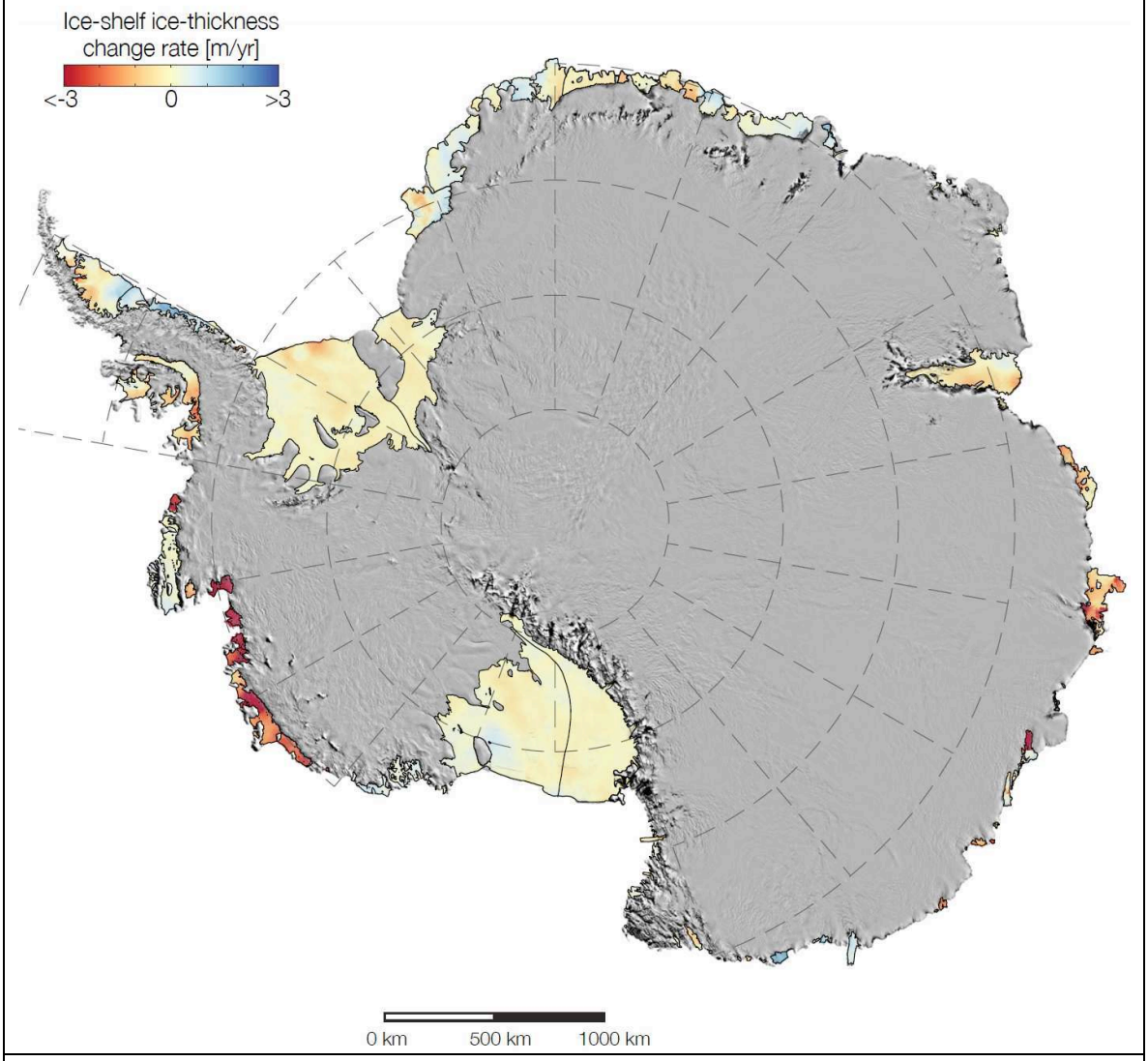

Figure S3. Antarctic ice shelf thickening $\partial H/\partial t$ for years 2003-2008 derived from ICESat-1 data using the methodology of *(23),* overlaid on a 2009 MODIS mosaic of Antarctica *(37).*

period 2003-2008 reduce the impact of this correction, which should not affect the results of this study.

We have no estimates of ice shelf thickening for a few ice shelves (Table S1). For Wordie and Ferrigno, we use the rates for the adjacent Wilkins and Venable shelves, respectively. Zero thickening is assumed for Lillie, Wilma/Robert/Downer, Rayner/Thyer, Edward VIII and Shirase in East Antarctica. Ice shelf thickening for Larsen B is based on measurements collected over the remnant part of the ice shelf.

§10. 'Steady-state' melt rates

Figure S4 shows the steady state melt rates, i.e. assuming zero thickening. This map may be compared with actual melt rates in Figure 1 and Table 1. Some ice shelves are close to equilibrium, some are thinning and accelerating, and others are thickening. The results

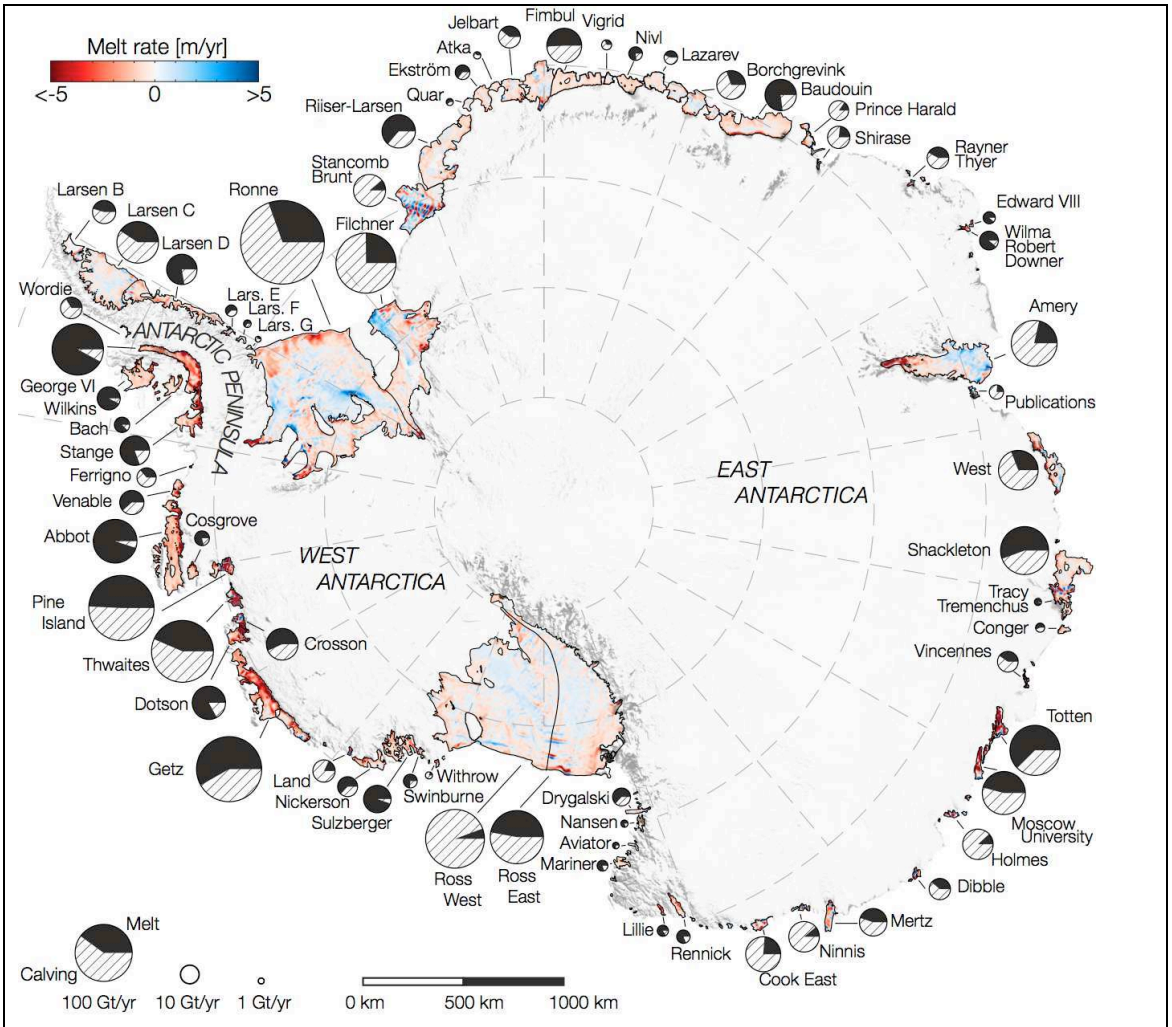

Figure S4. Antarctic map of steady state ice shelf melting rate with ice shelf names overlaid on a MOA mosaic of Antarctica. Pie charts denote 'steady-state' ice shelf melt water production in Gigatonnes per year (black) versus calving fluxes (hatched) as in Figure 1.

show that ice shelves melt and freeze in a complex fashion even when they are in state of mass equilibrium with the atmosphere and the ocean.

§11. Characteristics of Antarctic Ice Shelves (Table S1)

Table S1 (Excel Spreadsheet) includes the list of names, center location, GL flux, ice front flux, surveyed area, actual area, *SMB*, thickening and associated uncertainties for all surveyed ice shelves. We also list 34 smaller ice shelves not included in the survey, for a combined total of 7,425 square kilometer, or 0.5% of our total surveyed area. See footnotes and comments for additional details.

§12. Comparison with other studies (Table S2)

From 1962-1994, seven estimates of total Antarctic ice shelf area, excluding ice rises, have ranged from 1.381 – 1.570 million km^2 *(2, 3, 41).* Differences between those areas and our 1.561 million km^2 (Table S1) could result from decadal-scale ice front advance and retreat, along with larger uncertainties in grounding line and ice front positions in prior surveys. Substantial changes have occurred around the Antarctic Peninsula *(42).* Areas and area-averaged basal melt rates for individual ice shelves in this study (Tables 1 and S1) reflect ice front locations in 2007-2008.

A thorough comparison of our results with other estimates from ocean measurements, ocean modeling and glaciological methods is problematical because of the different and not always specified ice shelf and model domains. Additional complications include various assumptions about ice shelf thickness and cavity morphology, uncertainties regarding total melting versus net melting, different time frames for parameters known to evolve on seasonal to decadal scales, and extrapolations from limited measurements. There has also been a scarcity of reference data, or its use, although some models are tuned to ice divergence calculations. For example, Table S2 shows a wide variety of estimates for a large, slow-melting ice shelf (Filchner-Ronne) and for a small, fast-melting ice shelf (Pine Island). Their listed melt rates, in some cases converted to Gt/yr, may slight the cited studies, which often provide qualifications, error estimates, sensitivity analyses and evaluations of prior work.

We treat the Filchner and Ronne ice shelves separately because of their different source regions (EAIS and WAIS), melt rates and grounding line thicknesses. Most basal mass balance studies have combined the two, but a few have focused on one or the other, portions of the Ronne, or have provided information that allows a rough division. Here our separate results are combined for comparison, and the error bars should be noted in Table S1. It is readily apparent that full Filchner-Ronne estimates vary widely, and that ocean tides can be a substantial factor in modeling studies *(24).* Our combined results are higher than most prior estimates, including a study employing similar glaciological methods *(12),* and the large ice shelf area magnifies the Gt/yr equivalent of m/yr. The rate from *(6)* is mainly derived from a Ronne

glaciological transect *(15)* incorporating a high-melting zone near the grounding line and flanking the large region of basal freezing in Figure 1, plus a near- ice front estimate. The large negative outlier from satellite radar altimeter data *(45)* would be equivalent to basal freezing of 0.5 m/yr, and may be caused by a rise in the radar reflection horizon due to changes in the firn associated with melt events, as in *(46).*

Since the discovery of rapid melting of the Pine Island Ice Shelf in 1994 *(28),* most estimates of its melt rate have focused on the fast-moving extension of the Pine Island Glacier in its southern part. Estimates of that area have ranged from 2,000 – 3150 km^2, and adding the adjacent slow-moving shelf ice has raised the full area by as much as 300%. Even larger total ice shelf areas *(20*; Table S1*)* result in part from a retreat of the glacier grounding line. We assume that most estimates are for net melting, noting that *(45)* also reported a steady state rate (24 Gt/yr). Reported melt rates for the more active southern portion have ranged from 6 – 85 Gt/yr, and a rise over time would be consistent with observed changes in ocean forcing and cavity dimensions *(9).* The rate sensitivity to cavity shape in ocean modeling can be seen in *(29),* where full ice shelf average rates are 40% higher with OIB than with BEDMAP data. The low 13 Gt/yr rate was discounted by its authors, based on modeled 'warm' deep water in Pine Island Bay ~2°C colder than observed.

While our tables show melting rates in Gt/yr and m/yr, the spatial and temporal distribution of basal melting is more important than its sum or areal average. Near ice shelf grounding lines, e.g., the melting has a larger impact on mass balance and glacier flow into the sea. At several regions near incoming glaciers to the Filchner and Ronne ice shelves, grounding zone rates of 2–14 m/yr have been estimated from glaciological methods *(14),* and peak rates of 2.5–18 m/yr from ocean modeling *(24).* Under the Pine Island ice shelf, grounding zone rates have ranged from ~44 to >100 m/yr *(14, 47-48).*

Filchner and Ronne Ice Shelves						**Pine Island Ice Shelf**				
Date *(ref)*	Type	Area	Melt rate	Notes		Date *(ref)*	Type	Area	Melt rate	Notes
		km^2	Gt/yr					km^2	Gt/yr	
1984 *(49)*	GM	473,000	443			1983 *(58)*	GM	3,150	6	[4]
	GM	380,000	304	Ronne						
	GM	93,000	139	Filchner		1996 *(28)*	OO	3,000	28	[6]
1990 *(44)*	GT	530,000	126	[1]		1997 *(53)*	GM	2,500	28	
1992 *(06)*	GM	444,650	214	[2]		1998 *(54)*	OM	2,975	34	
1994 *(43)*	OO	500,000	46	[1]		1998 *(47)*	GM	2,000	22	
1998 *(50)*	OM	71,800	23	Filchner		2004 *(55)*	GM	2,365	33	
	GM	71,800	13	Filchner						
						2007 *(48)*	OM, GM	4,780	91	full ice shelf
1999 *(51)*	OM	450,000	37				OM, GM	3,010	81	
	OM	450,000	49							
	OM	450,000	11	[3]		2010 *(45)*	GM	6,000	33	full ice shelf
2001 *(10)*	OO	470,000	86			2011 *(56)*	GM	2,775	40	
2003 *(12)*	GM	533,333	83	[5]		2011 *(09)*	OO	2,450	78	
	GM	340,456	72	Ronne						
	GM	104,194	11	Filchner		2012 *(57)*	OM	?	101	[7]
2003 *(52)*	OO	470,000	146			2012 *(29)*	OM	3,026	58	Bedmap
							OM	3,026	84	OIB
2004 *(07)*	OM	408,000	120				OM	1,534	27	Bedmap
							OM	1,534	33	OIB
2010 *(45)*	GM	419,000	minus 206				OM	4,573	84	full Bedmap
							OM	4,573	118	full OIB
2011 *(24)*	OM	456,000	92	tidal forcing [5]						
		456,000	41	no tides [5]		2012 *(11)*	OM	5,000	13	full ice shelf
2012 *(11)*	OM	438,000	141	[4]						
THIS STUDY	GM	437,996	156			THIS STUDY	GM	5,920	101	full ice shelf
	GM	335,067	114	Ronne			GM	2,577	63	
	GM	102,929	42	Filchner						

GM = standard glaciological methods
OO = ocean observations
OM = ocean modeling
GT = geochemical tracers
OIB = Operation IceBridge

Table S2 notes:
For simplicity melt rates are rounded to the nearest integer, without infrequently provided error bars (e.g., ~30% in *(12, 52)*).
The comparisons above apply to the combined Filchner + Ronne and to the southern part of PIIS unless indicated otherwise.
Melt rates in Gt/yr have in some cases been converted from other units in the cited studies.
- [1] Based on meltwater content in 'Ice Shelf Water' seaward of ice shelves.
- [2] Extrapolated from 2-D section of *(15)* and modified by added area near ice fronts.
- [3] Simulation with no prescribed flow across ice front openings.
- [4] A much higher rate could be inferred from other information in text.
- [5] Area estimated; rate is total minus freezing.
- [6] Revised to 51 Gt/yr in *(9)*.
- [7] Full ice shelf area not specified within model domain of 9,720 km^2.

Table S2: Comparison of melt rates from other studies for Filchner and Ronne Ice Shelves, and for Pine Island Ice Shelf (PIIS)

§13. References

1. P. Fretwell *et al*., Bedmap2: Improved ice bed, surface and thickness datasets for Antarctica. *The Cryosphere* **7**, 375 (2013). doi:10.5194/tc-7-375-2013

2. C. W. Swithinbank, *Satellite Image Atlas of Glaciers of the World: Antarctica*, R. S. Williams, J. G. Ferrigno, Eds. (USGS Prof. Paper 1386-B, 1988).

3. N. I. Barkov, *Ice Shelves of Antarctica* (New Delhi, NY, Amerind Pub. Co., 1985).

4. R. LeB. Hooke, *Principles of Glacier Mechanics* (Cambridge University Press, Cambridge, 2005).

5. K. M. Cuffey, W. S. B. Paterson, *The Physics of Glaciers* (Elsevier, Burlington, MA, ed. 4, 2010).

6. S. S. Jacobs, H. H. Hellmer, C. S. M. Doake, A. Jenkins, R. M. Frolich, Melting of ice shelves and the mass balance of Antarctica. *J. Glaciol.* **38**, 375 (1992).

7. H. H. Hellmer, Impact of Antarctic ice shelf basal melting on sea ice and deep ocean properties. *Geophys. Res. Lett.* **31**, L10307 (2004). doi:10.1029/2004GL019506

8. A. Jenkins, S. S. Jacobs, Circulation and melting beneath George VI Ice Shelf, Antarctica. *Geophys. Res. Lett.* **113**, (C4), C04013 (2008). doi:10.1029/2007JC004449

9. S. S. Jacobs, A. Jenkins, C. F. Giulivi, P. Dutrieux, Stronger ocean circulation and increased melting under Pine Island Glacier ice shelf. *Nature Geosc.* **4**, 519 (2011). doi:10.1038/ngeo1188

10. A. Foldvik, T. Gammelsrod, E. Nygaard, S. Osterhus, Current measurements near Ronne Ice Shelf: Implications for circulation and melting. *J. Geophys. Res. Oceans* **106**, (C3), 4463 (2001). doi:10.1029/2000JC000217

11. R. Timmermann, Q. Wang, H. H. Hellmer, Ice-shelf basal melting in a global finite-element sea-ice/ice-shelf/ocean model. *Ann. Glaciol.* **53**, 303 (2012). doi:10.3189/2012AoG60A156

12. I. Joughin, L. Padman, Melting and freezing beneath Filchner-Ronne Ice Shelf, Antarctica. *Geophys. Res. Lett.* **30**, 1477 (2003). doi:10.1029/2003GL016941

13. J. Wen *et al*., Basal melting and freezing under the Amery Ice Shelf, East Antarctica. *J. Glaciol.* **56**, 81 (2010). doi:10.3189/002214310791190820

14. E. Rignot, S. S. Jacobs, Rapid bottom melting widespread near Antarctic Ice Sheet grounding lines. *Science* **296**, 2020 (2002). doi:10.1126/science.1070942 Medline

15. A. Jenkins, C. S. M. Doake, Ice ocean interaction on Ronne Ice Shelf, Antarctica. *J. Geophys. Res.* **96**, (C1), 791 (1991). doi:10.1029/90JC01952

16. J. T. M. Lenaerts *et al*., Modeling drifting snow in Antarctica with a regional climate model: 1. Methods and model evaluation. *J. Geophys. Res.* **117**, (D5), D05108 (2012). doi:10.1029/2011JD016145

17. E. Rignot *et al*., Recent mass loss of the Antarctic Ice Sheet from dynamic thinning. *Nat. Geosci.* **1**, 106 (2008). doi:10.1038/ngeo102

18. C. Allen, IceBridge MCoRDS L2 Ice Thickness. Boulder, Colorado USA: NASA DAAC at the National Snow and Ice Data Center (2010).

19. D. D. Blankenship, S. Kempf, D. Young, IceBridge HiCARS 2 L2 Geolocated Ice Thickness. Boulder, Colorado USA: NASA DAAC at the National Snow and Ice Data Center (2012).

20. J. A. Griggs, J. L. Bamber, Antarctic ice-shelf thickness from satellite radar altimetry. *J. Glaciol.* **57**, 485 (2011). doi:10.3189/002214311796905659

21. E. Rignot, J. Mouginot, B. Scheuchl, Antarctic grounding line mapping from differential satellite radar interferometry. *Geophys. Res. Lett.* **38**, L10504 (2011). doi:10.1029/2011GL047109

22. E. Rignot, J. Mouginot, B. Scheuchl, Ice flow of the Antarctic ice sheet. *Science* **333**, 1427 (2011). doi:10.1126/science.1208336 Medline

23. H. D. Pritchard *et al*., Antarctic ice-sheet loss driven by basal melting of ice shelves. *Nature* **484**, 502 (2012). doi:10.1038/nature10968 Medline

24. K. Makinson, P. R. Holland, A. Jenkins, K. Nicholls, D. M. Holland, Influence of tides on melting and freezing beneath Filchner Ronne Ice Shelf, Antarctica. *Geophys. Res. Lett.* **38**, L06601 (2011). doi:10.1029/2010GL046462

25. H. J. Horgan, R. T. Walker, S. Anandakrishnan, R. B. Alley, Surface elevation changes at the front of the Ross Ice Shelf: Implications for basal melting. *J. Geophys. Res.* **116**, (C2), C02005 (2011). doi:10.1029/2010JC006192

26. A. Shepherd *et al*., A reconciled estimate of ice-sheet mass balance. *Science* **338**, 1183 (2012). doi:10.1126/science.1228102 Medline

27. S. Neshyba, E. G. Josberger, On the estimation of Antarctic iceberg melt rate. *J. Phys. Oceanogr.* **10**, 1681 (1980). doi:10.1175/1520-0485(1980)010<1681:OTEOAI>2.0.CO;2

28. K. Grosfeld *et al*., Marine ice beneath Filchner Ice Shelf: Evidence from a multi-disciplinary approach. *Antarct. Res. Ser.* **75**, 319 (1998). doi:10.1029/AR075p0319

29. M. P. Schodlok, D. Menemenlis, E. Rignot, M. Studinger, Sensitivity of the ice shelf ocean system to the sub-ice shelf cavity shape measured by NASA IceBridge in Pine Island Glacier, West Antarctica. *Ann. Glaciol.* **53**, 156 (2012). doi:10.3189/2012AoG60A073

30. G. D. Williams *et al*., Late winter oceanography off the Sabrina and BANZARE coast (117–1281°E), East Antarctica. *Deep Sea Res. Part II Top. Stud. Oceanogr.* **58**, 1194 (2011). doi:10.1016/j.dsr2.2010.10.035

31. P. R. Holland, A. Jenkins, D. Holland, Ice and ocean processes in the Bellingshausen Sea, Antarctica. *Geophys. Res. Lett.* **115**, (C5), C05020 (2010). doi:10.1029/2008JC005219

32. L. Padman *et al*., Oceanic controls on the mass balance of Wilkins Ice Shelf, Antarctica. *J. Geophys. Res.* **117**, (C1), C01010 (2012). doi:10.1029/2011JC007301

33. P. R. Holland, H. F. J. Corr, D. G. Vaughan, A. Jenkins, P. Skvarca, Marine ice in Larsen Ice Shelf. *Geophys. Res. Lett.* **36**, L11604 (2009). doi:10.1029/2009GL038162

34. P. R. Holland, A. Jenkins, D. M. Holland, The response of ice shelf basal melting to variations in ocean temperature. *J. Clim.* **21**, 2558 (2008). doi:10.1175/2007JCLI1909.1

35. H. H. Hellmer, F. Kauker, R. Timmermann, J. Determann, J. Rae, Twenty-first-century warming of a large Antarctic ice-shelf cavity by a redirected coastal current. *Nature* **485**, 225 (2012). doi:10.1038/nature11064 Medline

36. T. A. Scambos, T. M. Haran, M. A. Fahnestock, T. H. Painter, J. Bohlander, MODIS-based Mosaic of Antarctica (MOA) data sets: Continent-wide surface morphology and snow grain size. *Remote Sens. Environ.* **111**, 242 (2007). doi:10.1016/j.rse.2006.12.020

37. R. A. Bindschadler *et al*., Getting around Antarctica: New high-resolution mappings of the grounded and freely-floating boundaries of the Antarctic Ice Sheet created for the International Polar Year. *The Cryosphere* **5**, 569 (2011). doi:10.5194/tc-5-569-2011

38. J. Mouginot, B. Scheuchl, E. Rignot, Mapping of ice motion in Antarctica using synthetic-aperture radar data. *Remote Sens.* **4**, 2753 (2012). doi:10.3390/rs4092753

39. R. J. Motyka, L. Hunter, K. A. Echelmeyer, C. Connor, Submarine melting at the terminus of a temperate tide-water glacier, LeConte Glacier, Alaska. *Ann. Glaciol.* **36**, 57 (2003). doi:10.3189/172756403781816374

40. E. Rignot, M. Koppes, I. Velicogna, Rapid submarine melting of the calving faces of west Greenland glaciers. *Nat. Geosci.* **3**, 187 (2010). doi:10.1038/ngeo765

41. A. J. Fox, A. Paul, R. Cooper, Measured properties of the Antarctic Ice Sheet derived from the SCAR Antarctic digital database. *Polar Rec. (Gr. Brit.)* **30**, 201 (1994). doi:10.1017/S0032247400024268

42. A. J. Cook, D. G. Vaughan, Overview of areal changes of the ice shelves on the Antarctic Peninsula over the past 50 years. *The Cryosphere* **4**, 77 (2010). doi:10.5194/tc-4-77-2010

43. T. Gammelsrød *et al.*, Distribution of water masses on the continental shelf in the southern Weddell Sea, in *The Polar Oceans and Their Role in Shaping the Global Environment, Geophys. Monogr. Ser.*, vol. 85, O. M. Johannessen, R. D. Muench, J. E. Overland (Eds.), pp. 159–176 (AGU, Washington, D. C., 1994), pp. 159–176; doi:10.1029/GM085p0159.

44. P. Schlosser *et al*., Oxygen 18 and helium as tracers of ice shelf water and water/ice interaction in the Weddell Sea. *J. Geophys. Res.* **95**, (C3), 3253 (1990). doi:10.1029/JC095iC03p03253

45. A. S. Shepherd *et al*., Recent loss of floating ice and the consequent sea level contribution. *Geophys. Res. Lett.* **37**, L13503 (2010). doi:10.1029/2010GL042496

46. R. H. Thomas *et al*., A comparison of Greenland ice-sheet volume changes derived from altimetry measurements. *J. Glaciol.* **54**, 203 (2008). doi:10.3189/002214308784886225

47. E. J. Rignot, Fast recession of a west Antarctic glacier. *Science* **281**, 549 (1998). doi:10.1126/science.281.5376.549 Medline

48. A. J. Payne *et al*., Numerical modeling of ocean-ice interactions under Pine Island Bay's ice shelf. *J. Geophys. Res.* **112**, (C10), C10019 (2007). doi:10.1029/2006JC003733

49. C. S. M. Doake, Glaciological Evidence: Antarctic Peninsula, Weddell Sea; *Glaciers, Ice Sheets, and Sea Level: Effect of a CO2-induced Climatic Change*, Seattle Workshop, Washington, 13-15 Sep 1984, USDOE/ER/60235-1, 197-209, (1985)

50. S. S. Jacobs, H. H. Hellmer, A. Jenkins, Antarctic ice sheet melting in the southeast Pacific. *Geophys. Res. Lett.* **23**, 957 (1996). doi:10.1029/96GL00723

51. R. Gerdes, J. Determann, K. Grosfeld, Ocean circulation beneath Filchner-Ronne Ice Shelf from three-dimensional model results. *J. Geophys. Res.* **104**, (C7), 15,827 (1999). doi:10.1029/1999JC900053

52. K. W. Nicholls *et al*., Water mass modification over the continental shelf north of Ronne Ice Shelf, Antarctica. *J. Geophys. Res.* **108**, (C8), 3260 (2003). doi:10.1029/2002JC001713

53. A. Jenkins, D. G. Vaughan, S. S. Jacobs, H. H. Hellmer, J. R. Keys, Glaciological and oceanographic evidence of high melt rates beneath Pine Island Glacier, West Antarctica. *J. Glaciol.* **43**, 114 (1997).

54. H. H. Hellmer, S. S. Jacobs, A. Jenkins, Oceanic erosion of a floating Antarctic glacier in the Amundsen Sea. *Antarct. Res. Ser.* **75**, 83 (1998). doi:10.1029/AR075p0083

55. A. Shepherd, D. Wingham, E. Rignot, Warm ocean is eroding West Antarctic Ice Sheet. *Geophys. Res. Lett.* **31**, L23402 (2004). doi:10.1029/2004GL021106

56. R. A. Bindschadler, D. G. Vaughan, P. Vornberger, Variability of basal melt beneath the Pine Island Glacier ice shelf, West Antarctica. *J. Glaciol.* **57**, 581 (2011). doi:10.3189/002214311797409802

57. P. Heimbach, M. Losch, Adjoint sensitivities of sub-ice-shelf melt rates to ocean circulation under the Pine Island Ice Shelf, West Antarctica. *Ann. Glaciol.* **53**, 59 (2012). doi:10.3189/2012/AoG60A025

58. T. Hughes, The Stability of the West Antarctic Ice Sheet: What has happened and what will happen, *Proceedings, Carbon Dioxide Research Conference: CO2, Science and Consensus*, Berkeley Springs Workshop, 19-23 Sep 1982, USDOE, 820970-021, DE-AC05-76OR00033, 021, IV.62 (1983).